ACS APPLIED MATERIALS & INTERFACES

Research Article

www.acsami.org

Efficient Polymer Solar Cells Fabricated on Poly(3,4-ethylenedioxythiophene):Poly(styrenesulfonate)-Etched Old Indium Tin Oxide Substrates

Moneim Elshobaki,[†,‡] James Anderegg,[§] and Sumit Chaudhary*[,†,∥]

[†]Department of Materials Science and Engineering, [§]Ames Laboratory, United States Department of Energy (U.S. DOE), and [∥]Department of Electrical and Computer Engineering, Iowa State University, Ames, Iowa 50011, United States

[‡]Physics Department, Mansoura University, Mansoura 35516, Egypt

Supporting Information

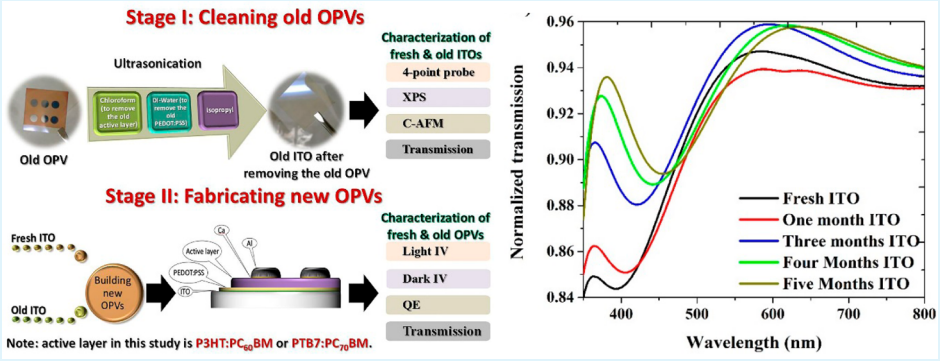

ABSTRACT: In organic electronic devices, indium tin oxide (ITO) and poly(3,4-ethylenedioxythiophene):poly(styrenesulfonate) (PEDOT:PSS) are the most common transparent electrode and anodic buffer layer materials, respectively. A widespread concern is that PEDOT:PSS is acidic and etches ITO. We show that this issue is not serious: only a few nanometers of ITO are etched in typical device processing conditions and storage thereafter; conductivity losses are affordable; and optical transmission gains further offset these losses. Organic photovoltaic (OPV) devices fabricated on old ITO (with PEDOT:PSS history) were similar or higher in efficiency than devices on fresh ITO. Poly[[4,8-bis[(2-ethylhexyl)oxy]benzo[1,2-*b*:4,5-*b*′]dithiophene-2,6-diyl][3-fluoro-2-[(2-ethylhexyl)carbonyl]thieno[3,4-*b*]thiophenediyl]] (PTB7) devices on old ITO showed efficiencies up to 9.24% compared to 8.72% efficient devices on fresh ITO. This reusability of ITO can be impactful for economics of organic electronics because ITO accounts for almost 90% of energy embedded in devices, such as OPVs.

KEYWORDS: *indium tin oxide, PEDOT:PSS, etching, polymer solar cells, transparent electrode*

INTRODUCTION

Owing to its high optical transmission and electrical conductivity, indium tin oxide (ITO) is the most popular transparent electrode in liquid crystal displays and optoelectronic devices. In organic electronic devices, such as organic photovoltaics (OPVs), ITO is widely used also because its work function is easily tuned by cleaning processes,[1] surface treatments,[2,3] and buffer layers.[4] Because indium is rare and demand for ITO is high, primarily in liquid crystal displays, prices of indium have been fluctuating.[5] This has led to efforts toward replacing ITO with new materials, such as metal nanowires, carbon nanotubes, graphene, and conductive polymers.[6] However, most alternatives are still inferior to ITO in overall performance. Replacements are also being sought for poly(3,4-ethylenedioxythiophene):poly(styrenesulfonate) (PEDOT:PSS), which is the most common anodic buffer layer in organic devices. PEDOT:PSS smoothens the surface, increases the work function of ITO for efficient collection (or injection) of holes,[7] and protects the overlying active layer from oxidative effect[8] of ITO. However, PEDOT:PSS is acidic and known to etch ITO,[9] thus, spurring research in alternatives, such as MoO_3,[10] NiO_x,[11] graphene oxide,[12] and V_2O_5.[13] Still, PEDOT:PSS remains the most popular anodic buffer layer and is a rather mature material; formulations of different conductivities are available for different applications. Motivated by our observation that an unencapsulated, ambient-stored, old ITO substrate-coated with PEDOT:PSS and other OPV layers can be cleaned and reused to fabricate efficient OPV devices, we investigated the impact of etching of ITO by PEDOT:PSS in detail. This paper discusses our several characterizations on this issue. Our key findings are that (1) PEDOT:PSS etches only a few nanometers of ITO,

Received: March 14, 2014
Accepted: July 21, 2014
Published: July 21, 2014

which does not seriously affect the charge collection and transport in OPV devices and (2) affordable conductivity losses are further offset by the gain in optical transmission of ITO, making PEDOT:PSS-etched ITO effective in increasing optical absorption in OPVs of promising contemporary materials, such as poly[[4,8-bis[(2-ethylhexyl)oxy]benzo[1,2-*b*:4,5-*b*′]-dithiophene-2,6-diyl][3-fluoro-2-[(2-ethylhexyl)carbonyl]-thieno[3,4-*b*]thiophenediyl]] (PTB7). Cleaning and reusing 2.5-year-old (PEDOT:PSS-coated) ITO, we fabricated 9.24% efficient OPV devices based on the PTB7 polymer compared to 8.72% efficient devices on fresh (new) ITO substrates. Considering that most OPVs currently have a lifetime of around 3−4 years,[14] suitable only for consumer electronic applications, it thus becomes unproblematic and even advantageous to continue using ITO and PEDOT:PSS and then reuse ITO from degraded or discarded OPVs to fabricate new batches. This can significantly impact the cost structure of OPVs; life cycle assessment has shown that ITO accounts for ∼90% of energy embedded in an OPV module.[15]

Although light has not been shed on the seriousness of etching, *prima facie*, there is no doubt that PEDOT:PSS etches ITO. It was shown using Rutherford backscattering technique that this etching initiates In diffusion in PEDOT:PSS, and diffusion saturates after a few days.[16] We probed the impacts of etching using several structural, electrical, and optical characterizations. OPV cells were also fabricated on old and fresh ITO substrates. Throughout this paper, old ITOs refer to ITO substrates that were coated with PEDOT:PSS/active layer/cathode and stored in ambient for the indicated amount of time or age and fresh ITOs refer to recently purchased ITOs with no PEDOT:PSS or device processing history. For all of the characterizations and refabrication on old ITOs, previously coated device layers were removed by typical ITO cleaning processes.

MATERIALS AND METHODS

Materials. P3HT, PTB7, $PC_{60}BM$, and $PC_{70}BM$ were purchased from 1-Material; ITO on glass (5−15 Ω/square) was purchased from Delta Technologies; and PEDOT:PSS (VP 4083) was purchased from HC Stark.

Solar Cell Fabrication. Device layers from old ITOs were removed by the sonication in chloroform. Both the fresh and old ITOs were further cleaned in detergent, deionized water, methanol, ethanol, and 2-propanol. After drying the ITO slides with N_2 on a hot plate at 150 °C for 15 min, they were exposed to high-dose air plasma for 5 min before depositing PEDOT:PSS (spin coating of 4000 rpm/60 s) and annealing at 150 °C for 30 min. Then, the substrates were transferred to a N_2-filled glovebox with oxygen and water levels less than 10 and 0.1 ppm, respectively. The P3HT:$PC_{60}BM$ blend (1:1, w/w; 10 mg/mL) was dissolved in *ortho*-dichlorobenzene by stirring overnight. The blend solution was filtered using plastic syringes and 0.2 μm filters, before spin coating the active layer at 500 rpm/40 s. P3HT:$PC_{60}BM$ cells had a structure of ITO/PEDOT:PSS (40 nm)/active layer/Ca (20 nm)/Al (100 nm) (see Figure S1 of the Supporting Information). Calcium and aluminum were thermally evaporated in a 10^{-6} mbar vacuum at rates less than 1 and 4 Å/s, respectively. For PTB7:$PC_{70}BM$ devices, the blend (1:1.5; 10 mg/mL) was dissolved by stirring overnight in mixed solvents (97% 1,2-dicholorobenzene and 3% 1,8-diiodooctane) and the active layer was spin-coated at 1000 rpm/60 s. The device structure was the same as P3HT:$PC_{60}BM$ cells. A total of 96 devices, each with an effective area of 0.1256 cm^2, were fabricated on fresh and used ITO substrates. Cells within a comparison set were fabricated on the same day using the same active layer solution.

Characterization of ITO Substrates and Solar Cells. The crystal structure and elemental composition of ITO were investigated using a Siemens D500 X-ray diffractometer and X-ray photoelectron spectroscopy (XPS), respectively. The current−voltage characteristics (1 sun) were obtained using an ELH Quartzline halogen lamp. External quantum efficiency was measured using a custom setup built from a single grating monochromator (Horiba Jobin Yvon), 100 W halogen bulb (OSRAM Bellaphot), and current pre-amplifier (Ithaco, Inc.). An optical chopper (Thor Laboratories) coupled with a lock-in amplifier (Stanford Research Systems) were used to reduce noise in the system. Optical absorption/transmission was measured in a Varian Cary 5000 ultraviolet−visible−near-infrared (UV−vis−NIR) spectrophotometer. Conductive atomic force microscopy (C-AFM) measurements were performed using Veeco Multimode Nanoscope III, and images were analyzed using Nanotec Electronica WSxM software.[17]

RESULTS AND DISCUSSION

ITO consists of a matrix of In_2O_3 and SnO_2. Because the atomic radii of Sn and In are comparable (0.71 and 0.81 Å, respectively), Sn substitutes In in the ITO matrix.[18] Thus, when the Sn concentration is increased, the ITO lattice constant decreases and its conductivity increases until a point, after which the dopants arrange interstitially and conductivity deteriorates.[19] Figure 1a shows the X-ray diffraction spectra of the fresh and some old ITO substrates. It is known that PEDOT:PSS etches In_2O_3 more than SnO_2;[9] this increases the

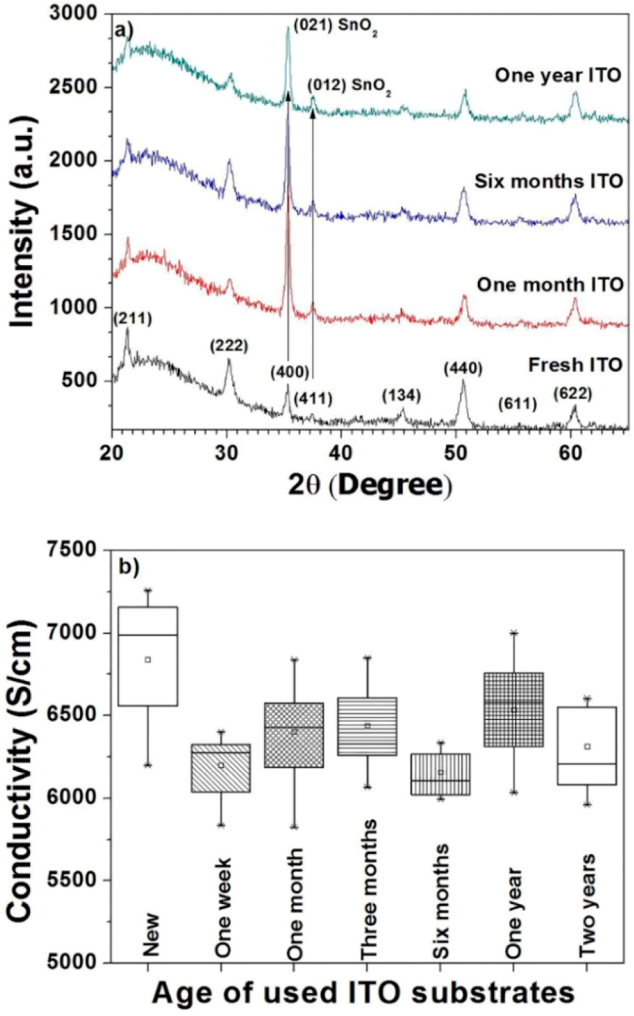

Figure 1. (a) X-ray diffraction spectra of fresh, 1-month-old, 6-month-old, and 1-year-old ITOs. (b) Conductivity boxplots of more than 30 old ITO substrates of different ages.

relative Sn content on the ITO surface and reduces the lattice constant of the (222) peak from 10.26 Å in fresh ITO to 10.21, 10.23, and 10.19 Å in the 1-month-old, 6-month-old, and 1-year-old ITO (see Figure S2a of the Supporting Information), respectively. At 2θ of 35.3° and 37.5°, the In_2O_3 (400) and (411) peaks seem to increase in old ITO. However, these peaks strongly overlap with the SnO_2 (021) and (012) peaks because of the comparable atomic radii of Sn and In and, thus, are also indicative of increased Sn content on the surface of old ITOs.

XPS showed that etching by PEDOT:PSS only changes the elemental composition of the top few nanometers (~5 nm) of the ITO film. As shown in Table 1 and panels b–d of Figure S2 of the Supporting Information, fresh ITO had higher In content or lower Sn/In ratio at the surface than 1-month-old, 6-month-old, and 1-year-old ITOs, in agreement with the X-ray diffraction results. However, after 5 min of Ar ion etching, which etches nearly 5 nm of ITO, elemental composition of fresh ITO was found to be similar to old ITOs (see values in parentheses in Table 1).

Table 1. Elemental Composition of the Fresh and Old ITOs before and after Ar Ion Etching, as Measured by XPS

	atomic concentration (%)[a]			
	O 1s	In 3d	Sn 3d	Sn/In ratio
fresh ITO	64.3	32.3	3.4	0.10
	(53.9)	(43.2)	(2.9)	(0.07)
1-month-old ITO	65.4	31.2	3.4	0.11
	(53.5)	(43.8)	(2.7)	(0.06)
6-month-old ITO	69.5	27.0	3.5	0.13
	(53.7)	(43.3)	(3.0)	(0.07)
1-year-old ITO	66.1	29.6	4.3	0.15
	(53.9)	(43.1)	(3.0)	(0.07)

[a]The values in parentheses are the atomic concentration of ITO constituents after surface etching.

Figure 1b shows the electrical conductivity box plots of fresh and several old ITOs, as measured by the four-point probe method. Overall, old ITOs exhibited lower conductivity, with variations being between −10 and +5% with respect to average conductivity of fresh ITO. To investigate morphology and conductivity at the nanoscale, we employed C-AFM. Morphology and current maps for fresh and old ITOs of three different ages are shown in panels a–h of Figure 2. Root-mean-square surface roughness decreased from 2.20 nm for the new ITO to 1.72, 1.48, and 1.69 nm for the 6-month-old, 1-year-old, and 2-year-old ITOs, respectively. This slight roughness decrease in old ITOs can be due to preferential etching of certain sharp features by PEDOT:PSS. Evidence of etching also appears in grain sizes, which are overall smaller in old ITOs. The C-AFM current maps were measured at an applied bias of +0.5 V. Root-mean-square current values of the fresh, 6-month-old, 1-year-old, and 2-year-old ITOs were 846, 227, 359, and 77 pA, respectively. It can be noted that, among the old ITOs, four-point probe and C-AFM measurements do not show a clear trend with the age of ITO. This can be due to different histories or manufacturing variabilities; the manufacturer itself specifies the sheet resistance of these ITOs to be not a precise number but in a range of 5–15 Ω/square. Fresh ITO, however, was notably different and more conductive than the old ITOs. This raises the question: if old ITOs are reused for OPV device fabrication, how do conductivity losses impact device performance?

To investigate this, we first fabricated and characterized poly(3-hexylthiophene-2,5-diyl):[6,6]-phenyl C_{61} butyric acid methyl ester (P3HT:PC_{60}BM)-based OPVs on fresh and some old ITO substrates. Figure 3a shows representative current–voltage characteristics, and Table 2 summarizes the performance parameters of these devices under 1 sun illumination. Owing to better fill factors, P3HT:PC_{60}BM OPVs on fresh ITO were slightly more efficient than the OPVs on old ITOs. Better fill factors in fresh ITO-based devices are ascribed to slightly

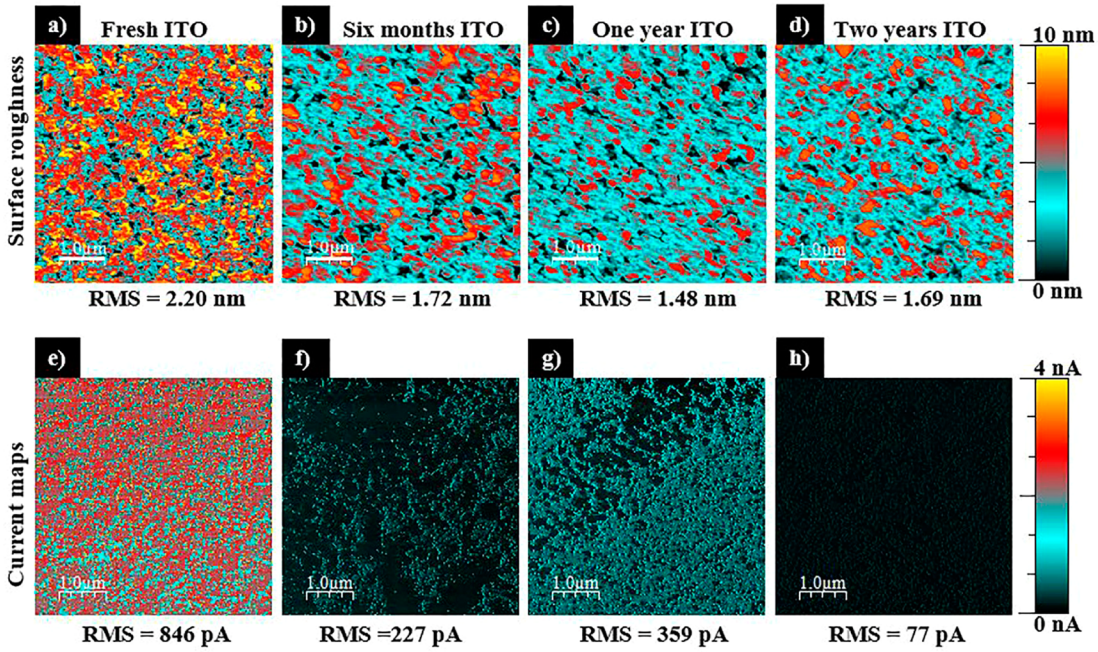

Figure 2. (a–d) C-AFM height and (e–h) current map images of the fresh and old ITO substrates. The current distribution images were captured at +0.5 V using a Pt–Ir-coated tip.

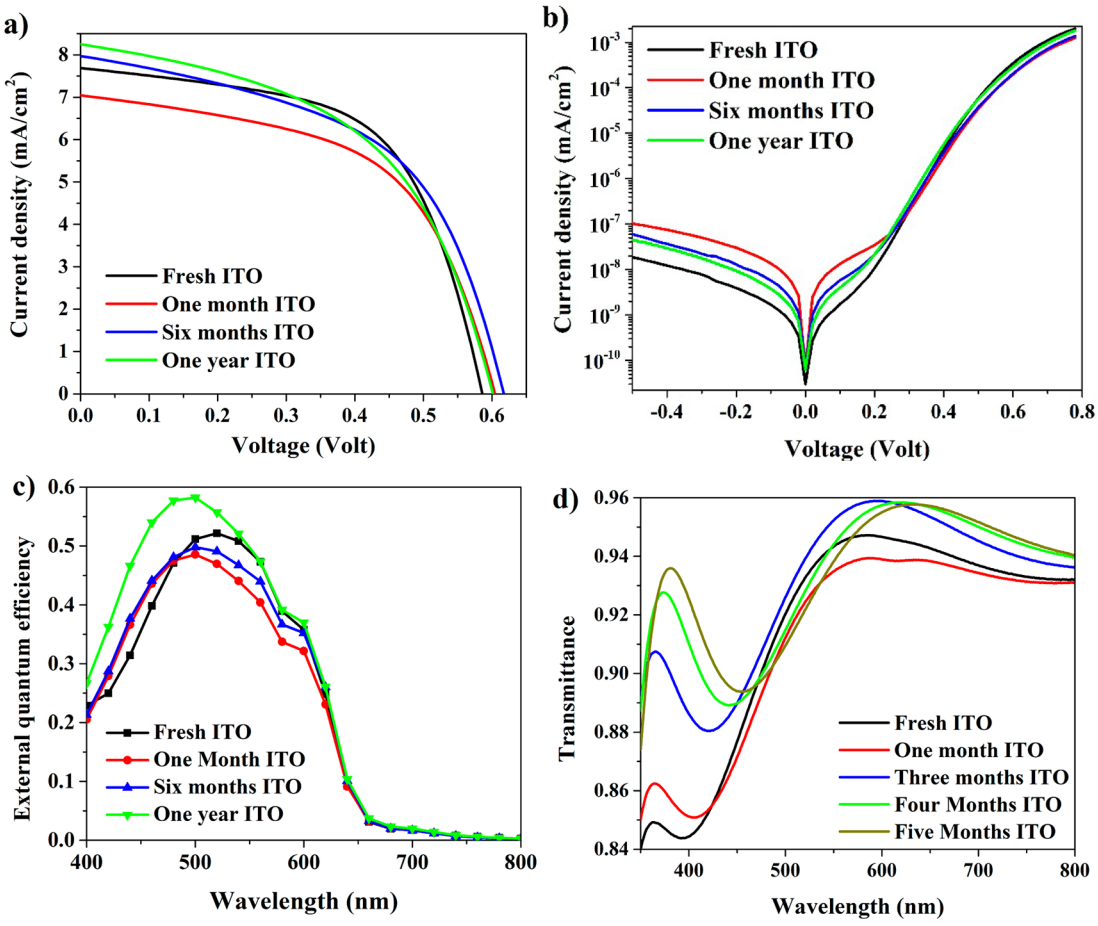

Figure 3. Current–voltage characteristics of P3HT:$PC_{60}BM$ OPVs (a) under illumination and (b) in the dark. (c) External quantum efficiency of P3HT:$PC_{60}BM$ OPVs. Shown current–voltage and quantum efficiency curves were from a single cell on a substrate containing six cells in total. Averages of all cells are presented in Table 2. (d) Optical transmission of fresh and old ITO substrates without any device layer.

Table 2. Photovoltaic Parameters of P3HT:$PC_{60}BM$ and PTB7:$PC_{70}BM$ Polymer Solar Cells

		V_{oc} (V)	J_{sc} (mA/cm^2)	FF (%)	η average (η_{best}) (%)
P3HT:$PC_{60}BM$	fresh ITO	0.59	7.62 ± 0.28	58	2.62 ± 0.10 (2.71)
	1-month-old ITO	0.61	6.98 ± 0.23	53	2.24 ± 0.15 (2.41)
	6-month-old ITO	0.61	7.79 ± 0.14	51	2.44 ± 0.18 (2.62)
	1-year-old ITO	0.60	7.93 ± 0.34	50	2.38 ± 0.12 (2.55)
PTB7:$PC_{70}BM$	fresh ITO	0.74	16.74 ± 0.37	69	8.55 ± 0.21 (8.72)
	1-month-old ITO	0.75	17.16 ± 0.52	69	8.82 ± 0.43 (9.04)
	6-month-old ITO	0.75	17.37 ± 0.37	70	9.07 ± 0.21 (9.24)
	1-year-old ITO	0.75	16.36 ± 0.66	70	8.50 ± 0.30 (8.78)
	fresh ITO	0.73	16.26 ± 0.62	63	7.30 ± 0.18 (7.63)
	30-month-old ITO	0.73	16.61 ± 0.56	64	7.66 ± 0.29 (8.17)

lower series resistance and higher shunt resistance; the latter also results in a decreased dark current in reverse bias, as shown by dark current–voltage characteristics (Figure 3b). Two surprising observations were as follows: (1) Of the three old ITOs used, devices fabricated on the two oldest ITOs showed higher short-circuit current (J_{sc}) than the fresh ITO-based devices. (2) External and normalized quantum efficiency curves for all of the old ITO-based devices were blue-shifted in comparison to the fresh ITO-based devices (Figure 3c and Figure S3 of the Supporting Information). To understand the reason behind this blue shift, we measured the transmission of our ITO substrates. Figure 3d shows that the old ITOs transmitted more light than fresh ITO in the 350–450 nm wavelength range and the transmission peak intensified with the increasing age of ITOs. This explains the quantum efficiency blue shift and J_{sc} enhancement in the case of old ITO-based devices and demonstrates that the conductivity loss in old ITOs is to some extent offset by the gain in visible-light transmission.

The transmission spectra of ITOs showed that, in addition to the 350–450 nm wavelength range, old ITOs also transmit more light in wavelengths around 600 nm and above. Old ITO-based P3HT:$PC_{60}BM$ devices did not benefit from this higher wavelength transmission enhancement because of low overlap with the P3HT absorption spectrum. However, emerging OPV materials, such as PTB7, do absorb these wavelengths in the red/NIR region; it is an important region where a significant

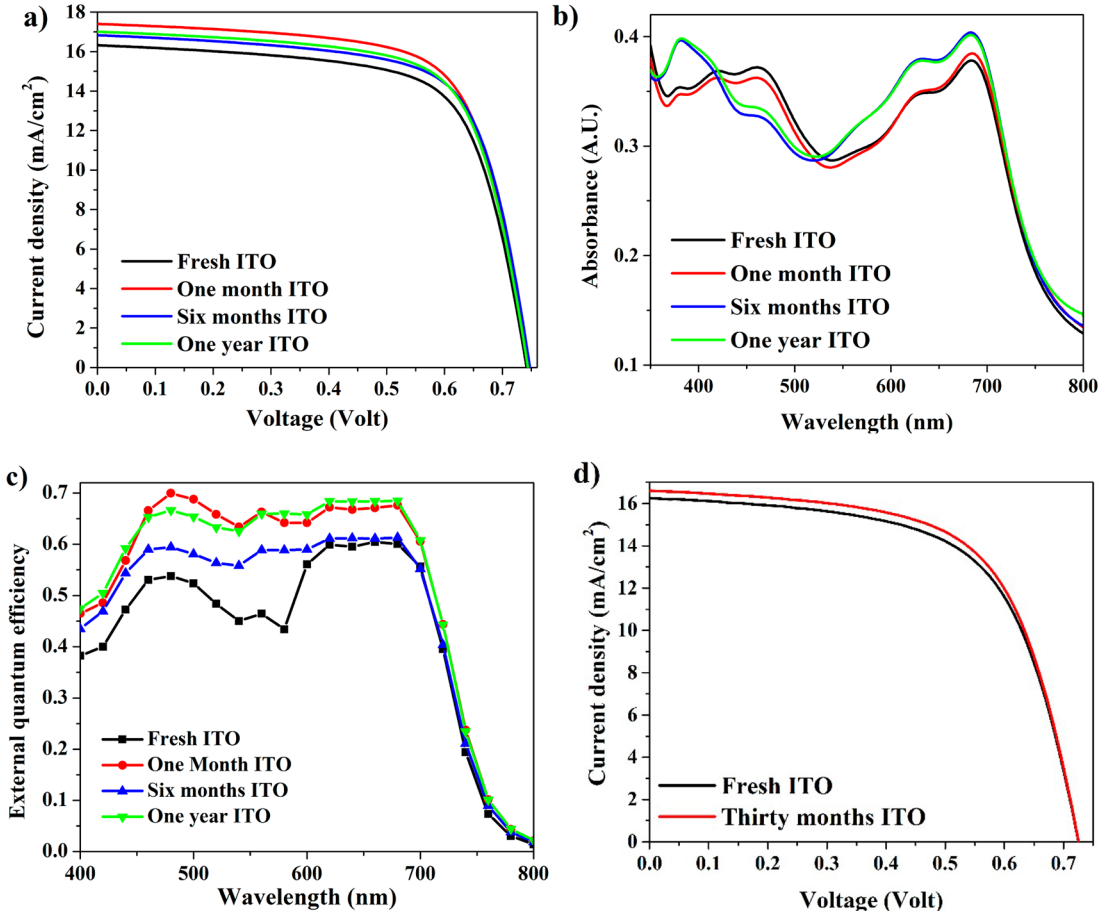

Figure 4. (a) Current–voltage characteristics of PTB7:$PC_{70}BM$ OPV devices under illumination, (b) absorbance of ITO/PEDOT:PSS/PTB7:$PC_{70}BM$ structures, and (c) external quantum efficiency of PTB7:$PC_{70}BM$ devices. Shown current–voltage and quantum efficiency curves were from a single cell on a substrate containing six cells in total. Averages of all cells are presented in Table 2. (d) Current–voltage characteristics of PTB7:$PC_{70}BM$ devices on the fresh and oldest ITO tested in this study.

amount of solar flux lies. Therefore, owing to its wide absorption range (400–750 nm), we chose and characterized the PTB7:$PC_{70}BM$ system on our fresh and old ITOs. Figure 4a shows representative current–voltage characteristics, and Table 2 summarizes the performance parameters of PTB7:$PC_{70}BM$ devices under 1 sun illumination. The fill factor of old ITO-based devices was similar to that of fresh ITO-based devices, showing that conductivity loss in the top few nanometers of ITO does not affect charge collection. However, results from PTB7:$PC_{70}BM$ clearly indicate that the near broadband transmission gain in old ITOs is notably beneficial. Devices based on 1-month-old and 6-month-old ITOs show on average 2.5 and 3.8% higher J_{sc}, respectively, than fresh ITO-based devices. The absorption spectra (Figure 4b) of PTB7:$PC_{70}BM$ films showed that, while absorption of fresh and 1-month-old ITO-based films are similar, films on older ITOs have higher absorption at lower and higher wavelengths, the same regions in which old ITOs transmit more than the fresh ITOs. External and normalized quantum efficiency curves (Figure 4c and Figure S4 of the Supporting Information) of PTB7:$PC_{70}BM$ devices show that the improved transmission of old ITOs notably contributes to photocurrent in these devices. The devices on 6-month-old ITO showed power conversion efficiency as high as 9.24%, which rivals the highest efficiencies in the PTB7:$PC_{70}BM$ system.[20] In another experiment, we also tested an even older ITO, 30-month-old ITO. PTB7:$PC_{70}BM$ devices fabricated on this 30-month-old ITO showed a 2% enhancement in J_{sc} over the fresh ITO-based devices; open-circuit voltage and fill factors were nearly the same (Figure 4d and Table 2). Considering that 30 months is approaching the current lifetime (3–4 years) of OPVs and that our old ITOs were ambient-stored rather than encapsulated, the prospect of reusing ITO from discarded OPV cells in consumer electronics clearly appears promising.

Lastly, we investigated whether buffer layers other than PEDOT:PSS can have a similar effect on ITO or not. We fabricated and characterized P3HT:$PC_{60}BM$ devices on old ITOs that were previously coated with different buffer layers, such as poly(9,9-bis(6′-((*N*,*N*,*N*-trimethyl)ammonium)hexyl)-2,7-fluorene) (PFN), molybdenum oxide (MoO_x), and cesium carbonate (Cs_2CO_3). PFN and Cs_2CO_3 are coated on ITO for inverted OPV cells in which ITO acts as a cathode, whereas MoO_x is a common anodic buffer layer like PEDOT:PSS. We found that old ITOs with MoO_x or PFN history were similar to fresh ITOs in terms of device performance and optical transmission (see panels a and b of Figure S5 of the Supporting Information). However, Cs_2CO_3 seems to also etch ITO like PEDOT:PSS, as we noted that devices fabricated on old ITOs with Cs_2CO_3 history showed (1) slightly higher short-circuit current than the fresh ITO-based devices and (2) slightly higher transmission in blue and associated blue shift in quantum efficiency of the device. In content on the surface

was also the least for ITO with Cs_2CO_3 history (see Table S1 of the Supporting Information). This apparent etching of ITO must be due to the basic nature of Cs_2CO_3. Surprisingly, the devices based on old ITOs with PFN history showed a quantum efficiency curve that was red-shifted in comparison to the fresh ITO-based devices (see Figure S5c of the Supporting Information); the reason for this is unclear, and further investigation is required.

CONCLUSION

In conclusion, we showed that the issue of ITO being etched by PEDOT:PSS is not a serious issue; only a few nanometers of ITO is etched, which does not hinder the charge collection, akin to the charge being easily able to tunnel through very thin insulating cathodic buffer layers, such as alkaline halides. These few nanometers of ITO etching in fact seem advantageous because it increases the ITO optical transmission by ∼10% in the blue/green region and 3% in the red/NIR region, which, in turn, leads to enhancement in the photocurrent of OPVs (that absorb these wavelengths) fabricated on the reused ITO substrates. Thus, reusing ITO from degraded and discarded OPV cells that include PEDOT:PSS is feasible and potentially impactful for the dollars/watt figure of merit.

ASSOCIATED CONTENT

Supporting Information

(i) Device structure of the fabricated solar cells, (ii) XPS spectra and results for both old and new ITO substrates, (iii) external quantum efficiency of P3HT:PC_{60}BM and PTB7:PC_{70}BM OPVs, (iv) photovoltaic characteristics, and (v) XPS results of P3HT:PC_{60}BM OPVs fabricated on fresh and old (previously coated with buffer layers other than PEDOT:PSS) ITO substrates. This material is available free of charge via the Internet at http://pubs.acs.org.

AUTHOR INFORMATION

Corresponding Author

*Telephone: 515-294-0606. Fax: 515-294-1152. E-mail: sumitc@iastate.edu.

Author Contributions

Moneim Elshobaki designed the experiment, fabricated and tested all of the devices, and analyzed the data. James Anderegg performed XPS characterization of ITO substrates. Sumit Chaudhary supervised the work, helped in the design of experiments, and co-wrote the paper with Moneim Elshobaki.

Notes

The authors declare no competing financial interest.

ACKNOWLEDGMENTS

This work was supported by the U.S. National Science Foundation (Award CBET 1236839). Moneim Elshobaki thanks the fellowship support from the Egyptian government under Contract GM915. The authors gratefully acknowledge John Carr, Max Noack, and Joydeep Bhattacharya for the fruitful discussions and help with providing old ITO substrates.

REFERENCES

(1) Sugiyama, K.; Ishii, H.; Ouchi, Y.; Seki, K. Dependence of indium-tin-oxide work function on surface cleaning method as studied by ultraviolet and X-ray photoemission spectroscopies. *J. Appl. Phys.* **2000**, *87*, 295−298.

(2) Brumbach, M.; Veneman, P. A.; Marrikar, F. S.; Schulmeyer, T.; Simmonds, A.; Xia, W.; Lee, P.; Armstrong, N. R. Surface composition and electrical and electrochemical properties of freshly deposited and acid-etched indium tin oxide electrodes. *Langmuir* **2007**, *23*, 11089−11099.

(3) Liau, Y.-H.; Scherer, N. F.; Rhodes, K. Nanoscale electrical conductivity and surface spectroscopic studies of indium−tin oxide. *J. Phys. Chem. B* **2001**, *105*, 3282−3288.

(4) Zhang, M.; Irfan; Ding, H.; Gao, Y.; Tang, C. W. Organic Schottky barrier photovoltaic cells based on MoO_x/C_{60}. *Appl. Phys. Lett.* **2010**, *96*, 183301.

(5) United States Geological Survey (USGS). Indium statistics and information. *Mineral Commodity Summaries*; USGS: Reston, VA, 2013; pp 74−75; http://minerals.usgs.gov/minerals/pubs/commodity/indium/mcs-2013-indiu.pdf.

(6) Angmo, D.; Krebs, F. C. Flexible ITO-free polymer solar cells. *Appl. Polym. Sci.* **2013**, *129*, 1−14.

(7) Huang, J.; Miller, P. F.; Wilson, J. S.; de Mello, A. J.; de Mello, J. C.; Bradley, D. D. C. Investigation of the effects of doping and post-deposition treatments on the conductivity, morphology, and work function of poly(3,4-ethylenedioxythiophene)/poly(styrene sulfonate) films. *Adv. Funct. Mater.* **2005**, *15*, 290−296.

(8) Scott, J. C.; Kaufman, J. H.; Brock, P. J.; DiPietro, R.; Salem, J.; Goitia, J. A. Degradation and failure of MEH-PPV light-emitting diodes. *J. Appl. Phys.* **1996**, *79*, 2745−2751.

(9) Wong, K. W.; Yip, H. L.; Luo, Y.; Wong, K. Y.; Lau, W. M.; Low, K. H.; Chow, H. F.; Gao, Z. Q.; Yeung, W. L.; Chang, C. C. Blocking reactions between indium-tin oxide and poly(3,4-ethylene dioxythiophene):poly(styrene sulphonate) with a self-assembly monolayer. *Appl. Phys. Lett.* **2002**, *80*, 2788−2790.

(10) Sun, Y.; Takacs, C. J.; Cowan, S. R.; Seo, J. H.; Gong, X.; Roy, A.; Heeger, A. J. Efficient, air-stable bulk heterojunction polymer solar cells using MoO_x as the anode interfacial layer. *Adv. Mater.* **2011**, *23*, 2226−2230.

(11) Steirer, K. X.; Ndione, P. F.; Widjonarko, N. E.; Lloyd, M. T.; Meyer, J.; Ratcliff, E. L.; Kahn, A.; Armstrong, N. R.; Curtis, C. J.; Ginley, D. S.; Berry, J. J.; Olson, D. C. Enhanced efficiency in plastic solar cells via energy matched solution processed NiO_x interlayers. *Adv. Energy Mater.* **2011**, *1*, 813−820.

(12) Li, S.-S.; Tu, K.-H.; Lin, C.-C.; Chen, C.-W.; Chhowalla, M. Solution-processable graphene oxide as an efficient hole transport layer in polymer solar cells. *ACS Nano* **2010**, *4*, 3169−3174.

(13) Zilberberg, K.; Trost, S.; Schmidt, H.; Riedl, T. Solution processed vanadium pentoxide as charge extraction layer for organic solar cells. *Adv. Energy Mater.* **2011**, *1*, 377−381.

(14) Peters, C. H.; Sachs-Quintana, I. T.; Kastrop, J. P.; Beaupre, S.; Leclerc, M.; McGehee, M. D. High efficiency polymer solar cells with long operating lifetimes. *Adv. Energy Mater.* **2011**, *1*, 491−494.

(15) Espinosa, N.; Garcia-Valverde, R.; Urbina, A.; Krebs, F. C. A life cycle analysis of polymer solar cell modules prepared using roll-to-roll methods under ambient conditions. *Sol. Energy Mater. Sol. Cells.* **2011**, *95*, 1293−1302.

(16) de Jong, M. P.; van IJzendoorn, L. J.; de Voigt, M. J. A. Stability of the interface between indium-tin-oxide and poly(3,4-ethylenedioxythiophene)/poly(styrenesulfonate) in polymer light-emitting diodes. *Appl. Phys. Lett.* **2000**, *77*, 2255−2257.

(17) Horcas, I.; Fernández, R.; Gómez-Rodríguez, J. M.; Colchero, J.; Gómez-Herrero, J.; Baro, A. M. WSXM: A software for scanning probe microscopy and a tool for nanotechnology. *Rev. Sci. Instrum.* **2007**, *78*, 013705.

(18) Warschkow, O.; Ellis, D. E.; González, G. B.; Mason, T. O. Defect structures of tin-doped indium oxide. *J. Am. Ceram. Soc.* **2003**, *86*, 1700.

(19) Pammi, S. V.; Chanda, A.; Ahn, J.-K.; Park, J.-H.; Cho, C.-R.; Lee, W.-J.; Yoon, S.-G. Low resistivity ITO thin films deposited by NCD technique at low temperature: Variation of tin concentration. *J. Electrochem. Soc.* **2010**, *157*, H937−H941.

(20) He, Z. C.; Zhong, C. M.; Su, S. J.; Xu, M.; Wu, H. B.; Cao, Y. Enhanced power-conversion efficiency in polymer solar cells using an inverted device structure. *Nat. Photonics* **2012**, *6*, 591−595.